



Two-Phase Risk Hedging Rules for Informing Conservation of Flood Resources in Reservoir Operation Considering Inflow Forecast Uncertainty

Bin Xu^{1,2}  · Xin Huang¹ · Ping-an Zhong¹ · Yanan Wu³

Received: 3 January 2020 / Accepted: 19 May 2020 /
Published online: 19 June 2020
© Springer Nature B.V. 2020

Abstract

Water shortages during dry periods can be successfully mitigated by managing reservoirs in real-time to conserve water as floods recede. The inherent uncertainty in inflow forecasts however means that it remains a challenge to balance the risks of flooding against those of water shortages. Few studies have examined how the risks of floods and water shortages can be managed using reservoir operation rules. In this study, a two-phase stochastic optimization model was built to determine the optimal conservation level for flood water by minimizing the risks from both floods and water shortages. For the optimal condition, hedging rules were analytically derived as a quasi-linear function of the storage capability and the expected water shortage. The rules indicate that the flood water conservation was achieved when the marginal upstream flood risk was equal to the marginal water shortage risk, and that the limits of three operation zones divided by the expected water availability should be used when determining the water release. The results from testing the model with data from the Xianghongdian Reservoir (China) showed that the hedging rules outperformed the capacity-constrained pre-release rules for conserving flood water without increasing the flood risk. This proposed methodology will inform the process for making decisions about how to operate reservoirs to ensure optimal real-time flood water conservation.

Keywords Reservoir operation · Flood water conservation · Hedging rules · Risky decision-making · First-order optimality condition

✉ Bin Xu
xubin_hhu@hhu.edu.cn

✉ Ping-an Zhong
pazhong@hhu.edu.cn

Extended author information available on the last page of the article

1 Introduction

In recent years, the conflict between the supply and demand for water resources in China has intensified drastically (Wen et al. 2018), to the extent that water resources are the main constraint on sustainable socioeconomic development in certain areas. Affected by the monsoon climate, the annual distribution of runoff to the principal rivers in the monsoon region of China (Liu and Shi 2019) varies considerably and exhibits high inter- and intra-annual variabilities. Highly variable inflows must be regulated by reservoirs (Mao et al. 2019) to maximize resource use and minimize loss during floods. Therefore, in an effort to alleviate the conflict between flood control and the water supply, it is thought that reservoirs could be operated to conserve flood water and mitigate water shortages (Shenava and Shourian 2018). Currently, the main objective of managing reservoirs during the flood season is to minimize the economic losses and social impacts caused by flood disasters (Moridi and Yazdi 2017) rather than conserve water. In this approach, the reservoir water level must be maintained below the flood limited water level (FLWL) to preserve flood storage before a flood occurs. With low levels of reservoir storage, it is thought that the spare capacity could be used to conserve flood water, reducing the waste of flood resources and using them to alleviate water shortages and improve ecological conditions. However, this conservation of flood water through reservoir operation rules is impeded by the lack of a technical method to determine a suitable conservation level, which ensures that the inherent uncertainty in the risks associated with flood control and water shortage are both acceptable and manageable (Xu et al. 2017).

Real-time reservoir operation formulates a risk decision-making problem that addresses uncertainty. A variety of optimization models, including explicit and implicit stochastic optimizations, have been developed to inform reservoir operation under uncertainty (Labadie 2004). Explicit stochastic optimization directly models uncertainty as stochastic processes and derives specific release and storage strategies (Yeh 1985; Yang et al. 2018). These models provide decision-making solutions but, because of their complexity, fail to explain the mechanism by which conflicting objectives interact and reach an optimum. This is widely recognized as a mathematical barrier that blocks the practical application of numerical optimization models. Implicit stochastic optimization, which obtains operating rules through data mining or analytical derivations based on optimal conditions (Lund and Guzman 1999), provides an alternative way to interpret the optimal conditions. In flood water conservation, Li et al. (2010) employed a capacity-constrained pre-release rule to determine that the upper limit of conservation could be as much as the pre-release capacity within an effective forecast lead-time. However, this rule fails to explicitly model the risks associated with forecast uncertainty, which could diminish the reliability of a strategy or give sub-optimal results.

Minimizing the total risks (Zhu et al. 2020) through reservoir operation by reallocating the temporal distribution of inflow involves formulating a risk hedging model (Bayazit and Unal 1990; Hashimoto et al. 1982). Analytical HRs, because of their ability to simplify the reservoir modelling operation into a two-phase (current and future phases) decision-making problem (Zhang et al. 2019), are considered advantageous for describing the optimization mechanism on the basis of the optimality principle. Various authors (Draper and Lund 2004; You and Cai 2008) used hydro-economic analysis to show that the optimal release followed the identical marginal utility regime (Zhao et al. 2011). At present, HRs have been widely used to investigate water supply (You and Cai 2008; Draper and Lund 2004; Shiao 2011), flood control (Zhao et al. 2014), reservoir refills (Wan et al. 2016; Ding et al. 2015), hydropower generation (Xu et al. 2017, 2019), and reservoir pre-release (Hui et al. 2016) operations.

Although various HRs for reservoir operation have been developed in previous studies, there is still a knowledge gap whereby the interactions between the risks of floods and water shortages are described by analytical formulae. Current HRs often address flood risks as the dominant index and determine the flood water conservation level without exceeding an acceptable level of flood risk. Using this approach, there could be over-conservation when the acceptable level of flood risk is high and the expected water shortages are low. Moreover, current HRs often assume a perfect foresight of inflow during the current phase, which potentially underestimate the occurrence probability of risks. The aim of this study therefore is to acknowledge and deal with the above knowledge gaps. The specific objectives of this study were (1) to develop a two-phase risk optimization model for conserving flood water during reservoir operation that explicitly represents flood risk and water shortage risk under uncertainties, (2) to derive analytical HRs that could characterize the optimal conservation decision based on the forecast inflow and forecast precision, and (3) to analyse the interactions between the risks of floods and water shortages under generic operating conditions.

2 Nomenclature

2.1 Abbreviations

| | |
|------|---------------------------------------|
| FLWL | Flood limited water level |
| CRs | Capacity-constrained pre-release rule |
| HRs | Hedging rules |
| FRs | Designed flood control rules |

2.2 Indices

i index of phase ($i = 1$, pre-refill phase; $i = 2$, pre-release phase).

2.3 Parameters

| | |
|----------------------------|---|
| T_i | the total number of time periods during phase i |
| Δt | the time interval in each time period (s) |
| V_u | the upper limit of storage for flood water conservation (m^3) |
| r_{\max} | the safety threshold of reservoir outflow (m^3/s) |
| τ | the effective lead-time of the forecasts based on hydrological forecasts (s) |
| R_i^u | the maximum water release without causing downstream flood inundation during phase i (m^3) |
| V_s | the beginning storage (m^3) |
| γ_a | the upper limit of the acceptable probability level of downstream flood risk. |
| ε_i | inflow forecast error during phase i , which is assumed unbiased and considered to obey a normal distribution, such that $\varepsilon_i \sim N(0, \sigma_{\varepsilon_i}^2)$ (m^3) |
| ε | total uncertainty of inflow forecast errors (m^3) |
| $\sigma_{\varepsilon_i}^2$ | variance of the forecast error ε_i (m^3) |

2.4 Functions

| | |
|-------------------------------------|--|
| $\omega_u[\cdot], \omega_d[\cdot],$ | damage functions of upstream flood risk, downstream flood risk and water |
| $\omega_s[\cdot]$ | shortage risk events. |
| $Prob(\cdot),$ | probability function and inverse function of a uncertain event. |
| $Prob^{-1}(\cdot)$ | |
| $p(\cdot)$ | is the probability density function for a normal distribution. |

2.5 Variables

| | |
|------------------------|---|
| \bar{q}_i | the forecast average inflow discharge(m ³ /s) |
| \bar{d}, \bar{D}_i | demand discharge (m ³ /s) and water (m ³) during phase i |
| V_i, \bar{V}_i | the actual and forecast (expected) ending storage (m ³) at phase i |
| I_i, \bar{I}_i | the actual and forecast inflow during phase i (m ³) i min, R_i max the lower and upper limits, respectively, of the actual or expected water release during phase i (m ³) |
| R_1 | deterministic water release decision during phase one (m ³) |
| R_2 | stochastic water release decision during phase one (m ³) |
| \bar{S}_2 | expected water shortage of pre-release phase (m ³) |
| SWA, EWA | hedging trigger range of expected water availability (m ³) |
| MWA | maximum expected water availability within feasible range (m ³) |
| R_i^c | the maximum water release capacity from all releasing facilities of the reservoir during phase i (m ³) |
| λ_1, λ_2 | the KKT multipliers of the storage lower and upper bound constraints. |
| $V_{1min},$ | the lower and upper limits of \bar{V}_1 (m ³). |
| V_{1max} | |

3 Methodology

The flowchart showing the framework of the coupling models that inform flood water conservation for deriving the analytical hedging rules is shown in Fig. 1. The general framework of the flood water conservation and the capacity-constrained pre-release rule (a benchmark rule) are introduced in Section 2.1. The concept and formulation of the hedging rules are introduced in Section 2.2. The two-phase optimal operation model is established, and the analytical derivation of the HRs based on the first-order optimality condition is presented, in Sections 2.3 and 2.4. Finally, the performance of the rules is examined under conditions with variable parameters and using real-time data from the Xianghongdian Reservoir, China.

3.1 Capacity-Constrained Pre-release Rules for Flood Water Conservation

As shown in Fig. 2, when a flood event is traced from its hydrograph, the regulation of the flood in a reservoir can be divided into three phases, namely pre-release, flood control, and pre-refill, depending on the inflow level. When flood water is conserved as a reservoir

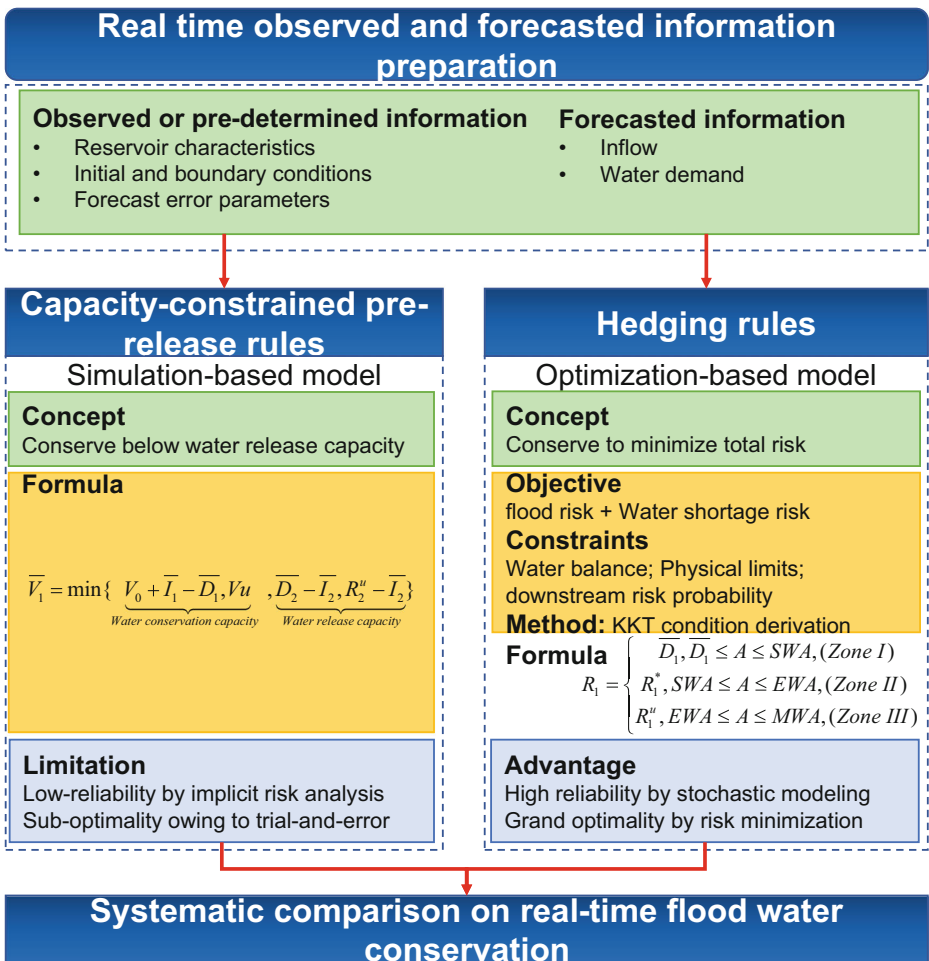


Fig. 1 Flow chart of the process for deriving the hedging rules

operation, water that is surplus to the water demand is stored during the pre-refill phase, and then is released to water users during the pre-release phase before the next flood occurs (Li et al. 2010). During the pre-refill phase, the average inflow discharge is predicted at \bar{q}_1 (m^3/s) above the demand discharge \bar{d} (m^3/s) ($\bar{q}_1 \geq \bar{d}$); this means that, when there is a water surplus, flood water would be conserved. In the pre-release phase, wherein the inflow discharge during dry periods is forecasted at the \bar{q}_2 (m^3/s) level below the demand discharge \bar{d} (m^3/s) ($\bar{q}_2 \leq \bar{d}$), the conserved flood water becomes a resource and can be delivered to mitigate water shortages.

Real-time flood water conservation decision-making depends on the forecast inflow during the pre-refill and pre-release phases. The upper bound of the flood conservation level should be determined jointly based on the water surplus ($V_0 + \bar{I}_1 - \bar{D}_1$), storage limit (Vu), water shortage ($\bar{D}_2 - \bar{I}_2$), and the maximum volume of water that can be released safely to the downstream river channel during the pre-release phase (R_2^u) (Chou and Wu

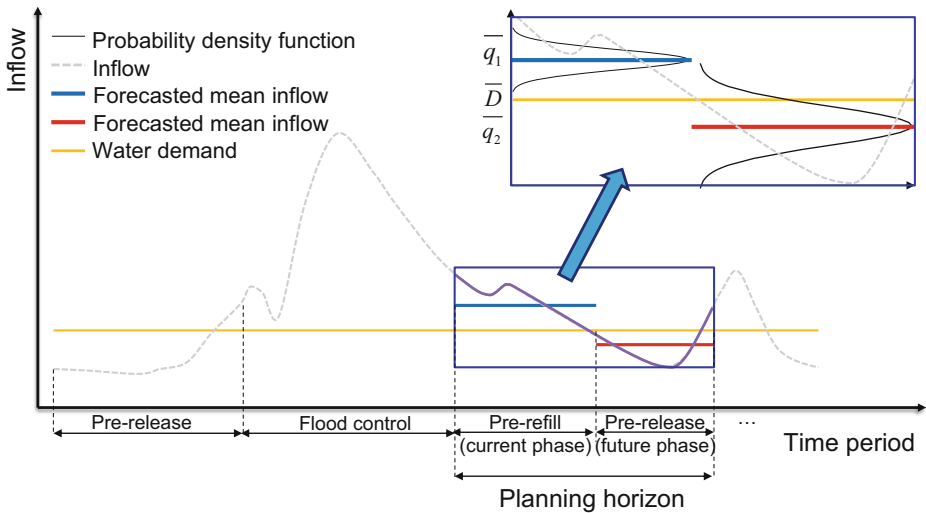


Fig. 2 Schematic of flood control and flood water conservation within a flood event

2013). This is characterized by the capacity-constrained pre-release method (Zhou et al. 2014; Li et al. 2010):

$$V_1 = \min \left\{ \underbrace{V_0 + I_1 - D_1, Vu}_{\text{Water conservation capacity}}, \underbrace{D_2 - I_2, R_2^u - I_2}_{\text{Water release capacity}} \right\} \tag{1}$$

$$\bar{I}_i = \bar{q}_i \cdot T_i \cdot \Delta t, \bar{D}_i = \bar{d} \cdot T_i \cdot \Delta t, R_i^u = r_{\max} \cdot T_i \cdot \Delta t, i = 1, 2 \tag{2}$$

The equations state that the final storage at the pre-release phase is controlled to the level of storage of the lower bound of the FLWL ($V_2 = 0$), such that flood water conservation does not lower the design standard of the reservoir in relation to flood control. To facilitate analysis, all storage variables refer to the relative storage level minus the storage below the FLWL.

Equation (1) indicates that the maximum conservation should neither exceed the water conservation capacity during the pre-refill phase nor surpass the water release capacity during the pre-release phase. Specifically, if $\min\{V_0 + \bar{I}_1 - \bar{D}_1, Vu, R_2^u - \bar{I}_2\} \geq \bar{D}_2 - \bar{I}_2$, then $\bar{V}_1 = \bar{D}_2 - \bar{I}_2$, demonstrating that a reasonable conservation equals as much as the expected water shortage ($\bar{D}_2 - \bar{I}_2$ or \bar{S}_2) of the pre-release phase, which is given as:

$$\bar{S}_2 = \bar{D}_2 - \bar{I}_2 \tag{3}$$

This method unfortunately fails to explicitly incorporate the influence of the inflow forecast error, thereby possibly increasing the risk and lowering the safety and reliability of the flood water conservation when operating reservoirs in real-time.

3.2 Hedging Rules

When the influence of the forecast uncertainty is addressed, flood water conservation through reservoir operation turns into a risky decision-making problem where the conflict between the risks of floods and water shortages need to be resolved, by determining the optimal

conservation level and decisions about release. Uncertainty in the inflow forecasts in the pre-refill phase and in the pre-release phase could result in the risks of floods and water shortages, respectively, with contradictions and transfers of massive balances between these two types of risks. To address this, reservoir release R_1 is introduced as a function (operation rule) of the expected available water A i.e., initial storage V_0 plus the forecast inflow \bar{I}_1 .

Among the different types of operation rules, HRs are typically useful for identifying trade-offs between releases and risks. HRs were first applied to rationalize inadequate water resources allocation between present and future stages, where the present water deliveries were curtailed and water was retained in storage for future use (Draper and Lund 2004). The hedging mechanism is used to reduce the risk of large shortages by allowing small shortages more frequently. By extending the hedging concept to model the flood water conservation rule, the conflict between the risks can be resolved. The HRs for flood water conservation through reservoir operation are shown in Fig. 3.

Within the feasible area of the chart, the blue upper bound of release corresponds to the minimal flood risk by releasing the maximum amount of water in phase one until R_1^u ; at the red lower bound of release, the water shortage risk is minimized by storing as much water as possible until it spills over. The HRs that intersect the two bounds separate the control of the release within the feasible area into three segments, as approximated by:

$$R_1 = \begin{cases} \overline{D_1}, \overline{D_1} \leq A \leq SWA, & (\text{Zone I}) \\ R_1^*, SWA \leq A \leq EWA, & (\text{Zone II}) \\ R_1^u, EWA \leq A \leq MWA, & (\text{Zone III}) \end{cases} \quad (4)$$

The HRs that guide release and conservation decisions are as follows:

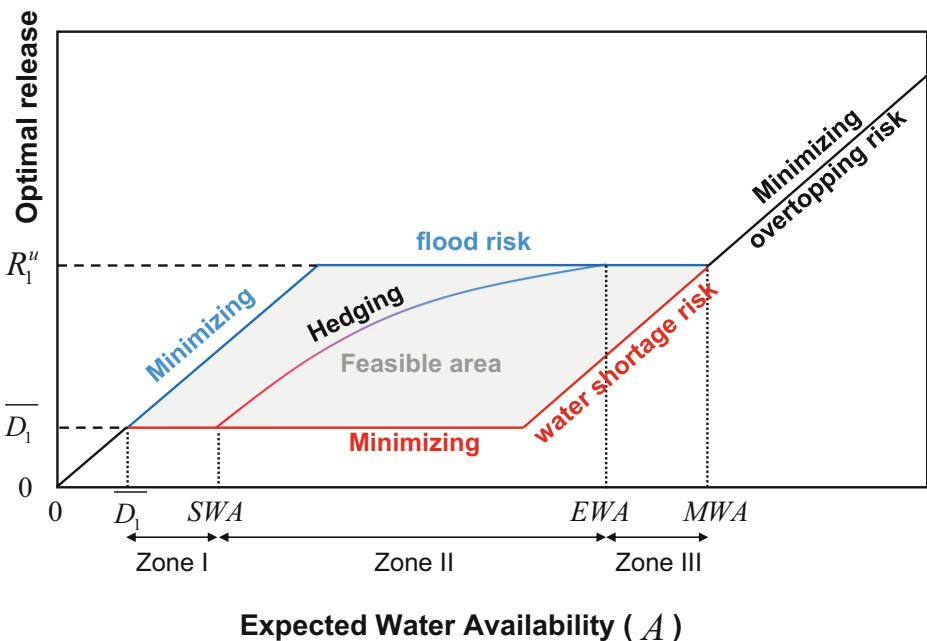


Fig. 3 Schematic of hedging rules on current release, where SWA and EWA denote the intersections of the hedging rule curve with the lower and upper bounds of water release, respectively

1. If A is within the range of $([\overline{D}_1, SWA])$ such that the flood risk is low and the water shortage risk is high, the release to \overline{D}_1 is limited and conservation is maximized to lower the water shortage risk;
2. If A is between the trigger range of hedging $([SWA, EWA])$ such that the flood risk balances the water shortage risk, the release to R_1^* is restricted and water is conserved at a medium level to achieve the best compromise;
3. Otherwise, A is in the range of $([EWA, MWA])$ such that the flood risk is high and the water shortage risk is low, and water is released to R_1^u to minimize the flood risk.

Clearly, HRs provide a solution for resolving the conflict between the risks by minimizing the total risk. Once the range threshold parameters of $[SWA, EWA, MWA]$ and release R_1^* are determined, the reservoir can be operated according to the rules by checking when and how hedging should be implemented.

3.3 Two-Phase Optimal Flood Water Conservation Model for Reservoir Operation

A two-phase optimal model that explicitly addresses the relationship between minimization of risks with flood water conservation was established in this study for deriving the HRs.

3.3.1 Defining the Risk

Inflow forecast uncertainty has been often identified as one of the primary sources of risk for real-time reservoir operation. It is characterized as the difference between the forecast inflow \overline{I}_i and the actual inflow I_i during phase i :

$$I_i = \overline{I}_i + \varepsilon_i, i = 1, 2 \tag{5}$$

Generally, the forecast error ε_i is assumed unbiased and considered to obey a normal distribution (Zhao et al. 2014) such that $\varepsilon_i \sim N(\mu_i, \sigma_{\varepsilon_i}^2)$ and $\mu_i = 0$. This assumption is acceptable because systematic forecast errors can frequently be corrected by subtracting the mean biases within real-time forecasts. The variance of the forecast error $\sigma_{\varepsilon_i}^2$ can be calibrated using the historical forecast and actual inflow samples.

1. Flood risk

The model determines a deterministic release decision in the current phase to guide the operation of power release and non-power release facilities. After making a deterministic release decision (R_1) during the current phase, the end storage adapts the forecast error in the inflow during this phase (ε_1), which could result in over-conservation of flood water (i.e., exceedance of the upper limit of conservation storage). This could result in damage within the drainage area of a reservoir or threaten the safety of a dam. Accordingly, the upstream flood risk is defined as the expected damage (L_u), which is the product of the probability (P_u) and the damage ($\omega_u [\overline{I}_1, \overline{I}_2]$):

$$L_u = P_u \cdot \omega_u = Prob(V_1 \geq Vu) \cdot \omega_u \tag{6}$$

Where $Prob(\cdot)$ is the probability function that evaluates the probability of a given uncertain event, and V_j is the actual end storage at the pre-refill phase that becomes a random variable when adapting ε_1 .

Note that $\omega_u[\cdot]$ is the damage function of the forecast inflow, which approximates to the estimation of the loss according to the return period of floods. The expression is later simplified by ω_u .

As the final storage at the pre-release phase is controlled to the storage of the lower bound of the FLWL ($V_2 = 0$), water release during the pre-release phase adapts the influence of both ε_1 and ε_2 . When meteorological forecasts fail to predict storm events that would occur during the pre-release phase, the amount of storm water to be released could be underestimated, meaning that it could exceed the maximum allowable water release to the downstream and cause downstream flood risk. The risk is defined as the expected flood inundation damage (L_d) to the downstream protection area and is calculated as follows:

$$L_d = Prob(R_2 \geq R_2^u) \cdot \omega_d \quad (7)$$

2. Water shortage risk

When there is uncertainty in the inflow forecast, the amount of water released during the pre-release phase may be insufficient to meet demand, such that water shortages occur, and the corresponding risk (L_s) is defined as the expected loss because of the shortage:

$$L_s = Prob(R_2 \leq \overline{D}_2) \cdot \omega_s \quad (8)$$

3.3.2 Model Formulation

To limit catastrophic damage in the downstream protected area from uncertainty and over-conservation, the downstream risk is formulated as a chance constraint by keeping the risk probability within an acceptable level. The other two risk indices are summed to establish the minimal total risk (Nayak et al. 2018):

(1) Objective function

$$\min L = \omega_u \cdot P_u + \omega_s \cdot P_s \quad (9)$$

(2) Constraints.

1) Water balance constraints:

$$V_1 = V_0 + I_1 - R_1; V_2 = V_1 + I_2 - R_2 \quad (10)$$

2) Chance constraint on the downstream flood risk probability:

$$Prob(R_2 \geq R_2^u) \leq \gamma_a \quad (11)$$

3) Water release limits:

$$R_1 \min \leq R_1 \leq R_1 \max \quad (12)$$

$$R_2 \min \leq \overline{R}_2 \leq R_2 \max \quad (13)$$

4) Initial and boundary storage conditions:

$$V_0 = V_s; V_2 = 0 \tag{14}$$

The specific values of the boundary limits given by Eqs. (12) and (13) can be determined from the physical limitations of the reservoir system as follows:

$$R_1 \min = \overline{D}_1; R_1 \max = \min\{R_1^u, R_1^c\}; \tag{15}$$

$$R_2 \min = 0; R_2 \max = R_2^u - \text{Prob}_{R_2}^{-1}(\gamma_a); \tag{16}$$

With given information on $\overline{I}_i, \sigma_{\varepsilon_i}^2, \overline{D}_i, Vu, V_s, R_i^u, \text{ and } R_i^c$ optimal decisions about R_1 can be derived analytically by solving the two-phase optimization model, yielding the HRs.

3.4 Analytical Solutions

The risk involved in flood water conservation stems from adaptation in relation to the forecast error during the two phases through reservoir storage and water release. The propagation of uncertainty can be verified through the following equations based on Eqs. (5), (10), and (14):

$$V_I = \underbrace{V_0 + I_1 - R_1}_{\overline{V}_1} + \varepsilon_I \tag{17}$$

$$R_2 = V_I - V_2 + I_2 + \varepsilon_2 = V_1 + \varepsilon_I - 0 + I_2 + \varepsilon_2 = \underbrace{V_1 + I_2}_{\overline{R}_2} + \underbrace{\varepsilon_I + \varepsilon_2}_{\varepsilon} \tag{18}$$

Where V_I adapts the variation of ε_1 and R_2 adapts the total uncertainty of ε from both phases. Accordingly, both V_I and R_2 are normally distributed such that $V_1 \sim N(\overline{V}_1, \sigma_{\varepsilon_1}^2)$ and $R_2 \sim N(\overline{R}_2, \sigma_{\varepsilon}^2)$. Assuming ε_1 and ε_2 are independent, we have $\varepsilon \sim N(0, \sigma_{\varepsilon}^2)$ and $\sigma_{\varepsilon}^2 = \sigma_{\varepsilon_1}^2 + \sigma_{\varepsilon_2}^2$.

3.4.1 Model Transformation

Using Eqs. (17) and (18), P_u and P_s can be expressed as functions of \overline{V}_1 as follows:

$$P_u = \text{Prob}(V_1 \geq Vu) = \int_{Vu - \overline{V}_1}^{+\infty} p(\varepsilon_1) d\varepsilon_1 \tag{19}$$

$$P_s = \text{Prob}(R_2 \leq \overline{D}_2) = \int_{-\infty}^{\overline{D}_2 - \overline{V}_1 - \overline{I}_2} p(\varepsilon) d\varepsilon \tag{20}$$

Accordingly, the objective function of the total risk L can be characterized as:

$$\min L = \omega_u \int_{Vu - \overline{V}_1}^{+\infty} p(\varepsilon_1) d\varepsilon_1 + \omega_s \int_{-\infty}^{\overline{D}_2 - \overline{V}_1 - \overline{I}_2} p(\varepsilon) d\varepsilon \tag{21}$$

The constraints on \bar{V}_1 can be specified as follows:

$$S.T. \quad V_1 \min \leq \bar{V}_1 \leq V_1 \max \tag{22}$$

where $V_1 \min$ and $V_1 \max$ are the lower and upper limits of \bar{V}_1 , respectively, which can be determined using the following equations based on Eqs. (10) and (15)–(16):

$$V_1 \min = \max \left\{ V_0 + \bar{I}_1 - R_1 \max, R_2 \min - \bar{I}_2 \right\} \tag{23}$$

$$V_1 \max = \min \left\{ V_0 + \bar{I}_1 - R_1 \min, R_2 \max - \bar{I}_2 \right\} \tag{24}$$

Therefore, the two-phase model is converted to a single-variable optimization model characterized by Eqs. (21) and (22), which can be solved using the first-order optimality condition, i.e., the Karush–Kuhn–Tucker (KKT) condition.

3.4.2 Optimal Condition

The KKT condition can be used to derive the optimal solution \bar{V}_1^* of the constrained optimization model, satisfying the following equations under feasible conditions:

$$\left. \frac{dL}{d\bar{V}_1} \right|_{\bar{V}_1 = \bar{V}_1^*} - \lambda_1 \cdot \left. \frac{d(\bar{V}_1 - V_1 \min)}{d\bar{V}_1} \right|_{\bar{V}_1 = \bar{V}_1^*} - \lambda_2 \cdot \left. \frac{d(V_1 \max - \bar{V}_1)}{d\bar{V}_1} \right|_{\bar{V}_1 = \bar{V}_1^*} = 0 \tag{25}$$

$$\lambda_1 \cdot (\bar{V}_1^* - V_1 \min) = 0, \lambda_2 \cdot (V_1 \max - \bar{V}_1^*) = 0, \lambda_1, \lambda_2 \geq 0 \tag{26}$$

Substituting P_u and P_s from Eqs. (19) and (20), respectively, into Eq. (25) gives the following:

$$\omega_u \cdot \left. \frac{\int_{v_u - \bar{V}_1}^{+\infty} p(\varepsilon_1) d\varepsilon_1}{\partial \bar{V}_1} \right|_{\bar{V}_1 = \bar{V}_1^*} + \omega_s \cdot \left. \frac{\int_{-\infty}^{\bar{D}_2 - \bar{V}_1 - \bar{I}_2} p(\varepsilon) d\varepsilon}{\partial \bar{V}_1} \right|_{\bar{V}_1 = \bar{V}_1^*} - \lambda_1 + \lambda_2 = 0 \tag{27}$$

In this equation, the terms of $\omega_u \cdot \frac{\partial P_u}{\partial \bar{V}_1}$ and $\omega_s \cdot \frac{\partial P_s}{\partial \bar{V}_1}$ are the marginal upstream flood risk and marginal water shortage risk due to flood water conservation, respectively. $\omega_u \cdot \frac{\partial P_u}{\partial \bar{V}_1}$ is non-negative, indicating the increased upstream flood risk of per unit conservation; $\omega_s \cdot \frac{\partial P_s}{\partial \bar{V}_1}$ is non-positive, denoting the decreased water shortage risk of per unit conservation. Clearly, the optimal conservation plan depends on the balance of the two terms.

Expanding Eq. (27) gives the following:

$$\omega_u \cdot \frac{1}{\sqrt{2\pi} \cdot \sigma_{\varepsilon_1}} e^{-\frac{\left(v_u - \bar{V}_1^* \right)^2}{2\sigma_{\varepsilon_1}^2}} - \omega_s \cdot \frac{1}{\sqrt{2\pi} \cdot \sigma_{\varepsilon}} e^{-\frac{\left(\bar{D}_2 - \bar{V}_1^* - \bar{I}_2 \right)^2}{2\sigma_{\varepsilon}^2}} = \lambda_1 - \lambda_2 \tag{28}$$

Based on the KKT condition, the solution of \bar{V}_1^* can be classified into the following three situations:

1. $\lambda_1 = 0, \lambda_2 > 0$. An increase in \bar{V}_1 reduces the total risk. Therefore, $\bar{V}_1^* = V_1 \max$ and the operation falls within zone I.
2. $\lambda_1 = \lambda_2 = 0$. \bar{V}_1^* is achieved by balancing the marginal risks. Therefore, $\bar{V}_1^* \in [V_1 \min, V_1 \max]$ and the operation falls within zone II.
3. $\lambda_1 > 0, \lambda_2 = 0$. An increase in \bar{V}_1 results in increasing of total risk. Therefore, $\bar{V}_1^* = V_1 \min$ and operation falls within zone III.

The solution of \bar{V}_1^* in situation 2) can be derived analytically. Moreover, when \bar{V}_1^* is kept below Vu for $\bar{V}_1^* \leq Vu$, such that the upstream flood risk is reasonable, the analytical solution of \bar{V}_1^* is characterized as follows:

$$\bar{V}_1^* = \frac{1}{2\sigma_{\varepsilon_2}^2} \left[-2\sigma_{\varepsilon_1}^2 \cdot \bar{S}_2 + 2\sigma_{\varepsilon}^2 \cdot Vu - \sqrt{\left[2\sigma_{\varepsilon_1}^2 \cdot \bar{S}_2 - 2\sigma_{\varepsilon}^2 \cdot Vu \right]^2 - 4\sigma_{\varepsilon_2}^2 \cdot \left[-\sigma_{\varepsilon_1}^2 \cdot \bar{S}_2^2 + \sigma_{\varepsilon}^2 \cdot Vu^2 - 2\sigma_{\varepsilon_1}^2 \sigma_{\varepsilon}^2 \cdot \ln \left(\frac{\omega_u \cdot \sigma_{\varepsilon}}{\omega_s \cdot \sigma_{\varepsilon_1}} \right) \right]} \right] \tag{29}$$

Equation (29) implies that \bar{V}_1^* is a quasi-linear function of Vu and \bar{S}_2 . Moreover, \bar{V}_1^* is correlated negatively with $\frac{\omega_u}{\omega_s}$, demonstrating that the expected conservation level decreases if the relative ratio of flood damage divided by water shortage damage increases.

After obtaining \bar{V}_1^* from the analytical solution, the optimal solution for R_1 can be determined by replacing \bar{V}_1^* back to the water balance equation. Thereafter, the HRs characterized in Eq. (4) can be derived.

4 Overview of the Xianghongdian Reservoir System

The Pi River Irrigation District is located on one of the tributaries of the Huai River. It is part of China’s second largest irrigation district—the Pishihang Irrigation District—and has a total irrigation area of 73.33×10^4 hm². The primary irrigation water is delivered from a multi-reservoir system that includes the Xianghongdian, Bailianya, Mozitan, and Foziling Reservoirs, which are all on the upstream reaches of the Pi River (Fig. 4). Irrigation water is mainly delivered from May to October, between which the rice growing season and the flood season occur in the reservoir system. The demand for irrigation water peaks during dry inflow periods in July and August after the monsoon rains. The design reliability of irrigation water supply is 80%; however, the actual reliability is 73% and the water resource use efficiency is only 50%. On the other hand, the annual water shortage is estimated at 1.45×10^8 m³.

The Xianghongdian Reservoir, with a storage capacity of 26.32×10^8 m³, is the largest of the reservoirs in the Huai River Basin. By reserving a flood control storage of 4.76×10^8 m³, it ensures the safety of the downstream protected area of Lu’an and other metropolitan regions along the Huai River during times of flood. Supported by rainfall and flood information monitoring and forecasting systems with real-time responses, the reservoir system can forecast

the receding inflow with a 5-day lead-time. The technical parameters of the Xianghongdian Reservoir are provided in Table 1.

A matrix for calculating $\frac{\omega_{jt}}{\omega_s}$ with \bar{I}_1 and \bar{I}_2 is adopted to evaluate the risk of damage. The relevant data were provided by the operation management centre of the Xianghongdian Reservoir (Hua et al. 2020).

5 Results

5.1 Flood Water Conservation Results from Different Rules

The operation of the Xianghongdian Reservoir during the flood season is guided by phase-wise flood control rules (FRs) that determine the volume of water release relative to the current storage level and the current inflow condition. The FRs consider only flood control that protects areas upstream and downstream of the reservoir, and do not allow for flood water conservation above the FLWL after a flood recedes. The CRs consider a certain level of flood water conservation based on forecast information, but they fail to incorporate bias information and do not explicitly account for risk. Both sets of rules are selected as benchmarks for highlighting the differences in the results obtained using HRs.

The inflows forecast for the pre-refill and pre-release phases of three flood events were selected from historical records. Numerical simulations based on the derived rules were conducted within the MATLAB2018b platform. Statistics of the results achieved under the three sets of rules are compared in Table 2.

The results indicate the following.

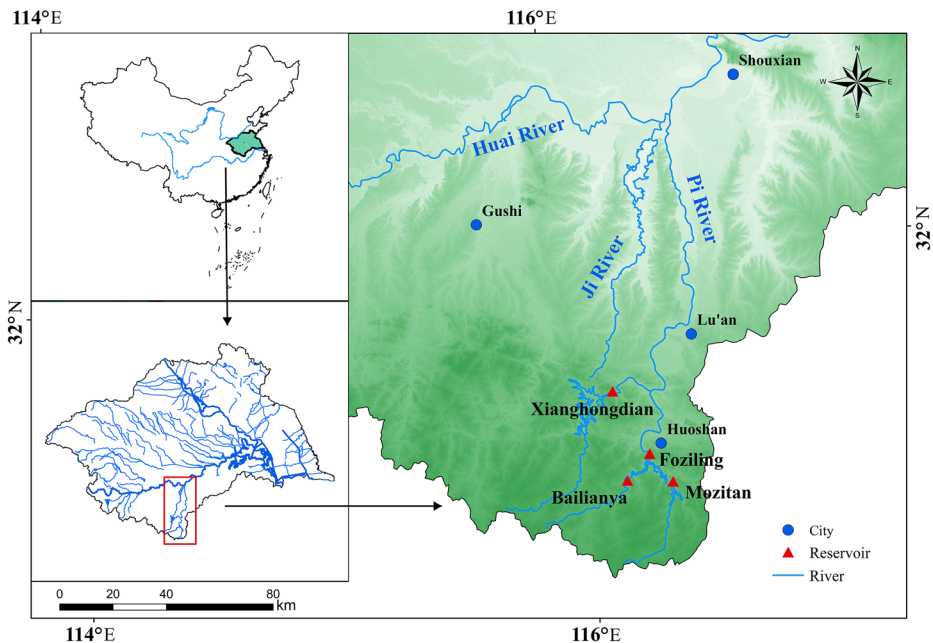


Fig. 4 Sketch map showing the location of the multi-reservoir system in the Pi River basin

Table 1 Parameters of flood control and water supply operation for the Xianghongdian reservoir

| T_1 (h) | T_2 (h) | $\sigma_{\varepsilon_1}(10^8\text{m}^3)$ | $\sigma_{\varepsilon_2}(10^8\text{m}^3)$ | \bar{d} (m ³ /s) | V_u (10^8m^3) | $R_{i,\text{min}}(10^8\text{m}^3)$ | $R_{i,\text{max}}(10^8\text{m}^3)$ | γ_a |
|-----------|-----------|--|--|-------------------------------|----------------------------|------------------------------------|------------------------------------|------------|
| 9 | 120 | 0.385 | 0.459 | 60 | 1.86 | 0.019/0 ^a | 0.204/1.177 | 0.5% |

^a The two values denote the results of phase I and phase II

1. Of all the rules tested, the HRs result in the smallest total risk by conserving the optimal level of flood water. Relative to the feasible range of \bar{V}_1 , HRs conserve the maximum level of flood water in case I, wherein P_s dominates P_u , an intermediate level in case II to reach the optimal equilibrium, and a minimum level in case III so that P_u is lowered.
2. Both the FRs and the CRs result in insufficient flood water use for addressing the dominating impact of flood control and flood risk. The conservation level associated with the two sets of rules is bound at the lower limit for case II and case III.

The results of the risks and the weighted marginal risks from the HRs under case I are plotted in Fig. 5.

Figure 5 clearly shows that the effect of water shortage risk gradually weakens as \bar{V}_1 increases and eventually becomes dominated by the flood risk. For the cases, the intersection point between $\omega_s \cdot \left| \frac{\partial P_s}{\partial V_1} \right|$ and $\omega_u \cdot \frac{\partial P_u}{\partial V_1}$ is $0.72 \times 10^8 \text{ m}^3$ and it decreases with $\frac{\omega_u}{\omega_s}$. Moreover, $\bar{V}_1^* \geq \bar{S}_2$ and the HRs outperform the CRs in terms of flood water conservation.

5.2 Results of Real-Time Operation within a Rolling Horizon

The performances of the three operating rules (i.e., FRs, CRs, and HRs) were investigated when applied to guide real-time operations within a rolling horizon during the flood season of 2015 and 2016. Model simulations were conducted with current statistical levels of forecast precision, using a 1-h time interval to reflect the hydrological variability. The executed water release for the current hour was determined as a proportion of the total water release during the pre-refill phase, and the proportion can be determined by the ratio of the forecast inflow during the current hour divided by the total forecast inflow during the pre-refill phase.

Forecast real-time inflow sequences were obtained from the forecast systems established at the operation centre of the reservoir. Eight indices (Shiau 2011) for assessing real-time reservoir operation performance during periods of flood and drought were considered: total water delivery (TWD), water supply reliability (WSR), maximum 10-day shortage ratio (MSR), total water spillage (TWS), chance of water spillage (CWS), maximum storage (MS), maximum outflow (MO), and end storage (ES). Statistics of these indices are listed in Table 3.

The results verify the following observations:

1. HRs conserve a higher level of flood water and ensure better water delivery than both the FRs and the CRs. For the HRs, the TWD were $0.5 \times 10^8 \text{ m}^3$ (6.3%) and $0.26 \times 10^8 \text{ m}^3$ (3.6%) higher, the WSR were 7.1% and 5.8% higher, and the MSR was 4.5% and 1.2% lower than the results of the CRs in 2015 and 2016, respectively. This is because the HRs determine the optimal conservation level for the expected water shortage and also use information about the probability and damage to rationalize operation.

Table 2 Statistics of the results achieved under different operating rules for three typical flood events

| Inflow cases | Operating rules | \bar{T}_1 (10 m) 8^3 | \bar{T}_2 (10 m) 8^3 | $\frac{w_2}{w_1}$ | R_1 (10 ⁸ m ³) | \bar{V}_1^* (10 m) 8^3 | $[V_1^{min}, V_1^{max}]$ (10 ⁸ m ³) | P_d | P_u | P_s |
|--------------|-----------------|-----------------------------|-----------------------------|-------------------|---|-------------------------------|--|----------|----------|----------|
| Case I | FRs | 0.3 | 0.2 | 18.24 | 0.2 | 0.1 | [0.1,0.28] | 2.64E-05 | 2.46E-06 | 4.73E-01 |
| | CRs | | | | 0.04 | 0.26 | | | 1.64E-05 | 3.69E-01 |
| | HRs | | | | 0.02 | 0.28 | | | 2.06E-05 | 3.56E-01 |
| Case II | FRs | 0.8 | 0.18 | 28.63 | 0.2 | 0.6 | [0.6,0.78] | 5.92E-04 | 5.37E-04 | 1.93E-01 |
| | CRs | | | | 0.2 | 0.6 | | | 5.37E-04 | 1.93E-01 |
| | HRs | | | | 0.08 | 0.72 | | | 1.54E-03 | 1.43E-01 |
| Case III | FRs | 1.2 | 0.1 | 49.18 | 0.20 | 1.00 | [1,1.18] | 2.01E-03 | 1.28E-02 | 8.06E-02 |
| | CRs | | | | 0.20 | 1.00 | | | 1.28E-02 | 8.06E-02 |
| | HRs | | | | 0.20 | 1.00 | | | 1.28E-02 | 8.06E-02 |

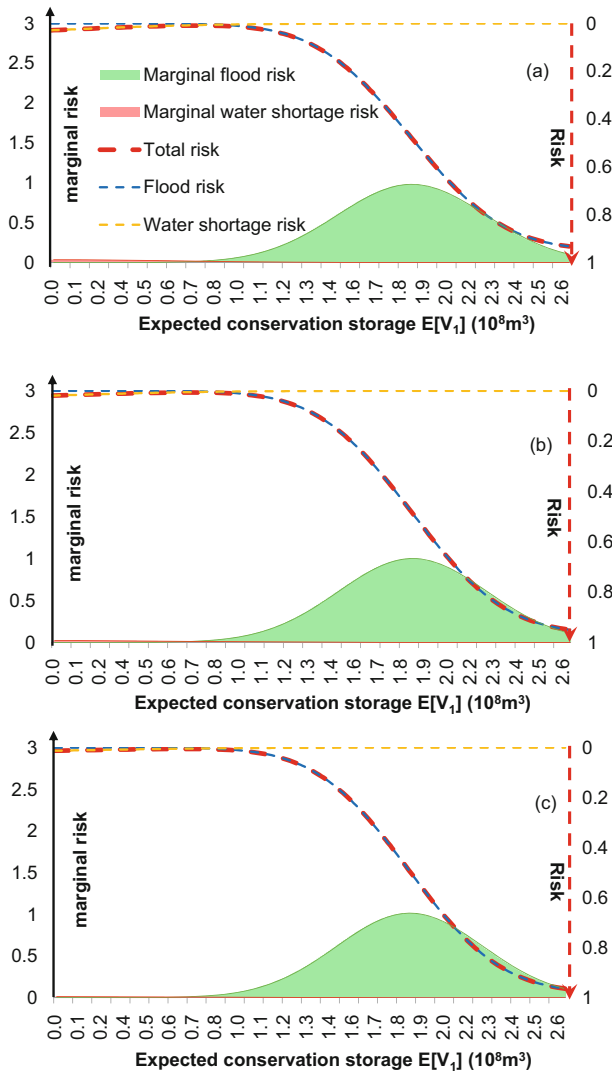


Fig. 5 Risks and marginal risks for (a) case I, (b) case II and (c) case III

2. Informed decisions on flood water conservation guided by the HRs do not necessarily increase the flood risk. The MS for the HRs ($0.91 \times 10^8 \text{ m}^3$) was higher than that for the FRs in 2015, but the storage level was much less than the upper boundary of flood storage; this ensured adequate safety for controlling floods. In 2016, the MS for the HRs was $0.13 \times 10^8 \text{ m}^3$ lower than that for the FRs, and the upstream flood risk was lower. The MO results from both the HRs and the FRs were the same, which indicates that real-time operation of HRs did not increase the downstream flood risk. This is because the HRs explicitly addressed the flood control risk as an objective and as a constraint for limiting the likelihood of flood occurrences, thereby preventing the severity of the risk when conserving flood water.

Table 3 Simulated statistics of indices from real-time operation strategies under different operating rules

| Year | Rules | TWD (10^8m^3) | WSR (%) | MSR (%) | TWS (10^8m^3) | CWS (%) | MS (10^8m^3) | MO (m^3/s) | ES (10^8m^3) |
|------|-------|-----------------------------|-----------------|-----------------|-----------------------------|-----------------|-------------------------------|------------------------------|----------------------------|
| 2015 | FRs | 7.55 | 59.1 | 79.6 | 2.49 | 15.6 | 0.47 | 630 | -0.814 |
| | CRs | 7.82 (3.6%) ^b | 69.5 (10.4%) | 78.5 (-1.1%) | 2.37 (-4.8%) | 10.4 (-5.2%) | 0.36 (-23.4%) | 1100 (74.6%) | -0.813 (-0.1%) |
| | HRs | 8.32 (6.3%) ^c | 76.6 (7.1%) | 74.1 (-4.5%) | 2.21 (-6.8%) | 15.6 (5.2%) | 0.91 ^a (152.8%) | 630 (-42.7%) | -0.808 (-0.6%) |
| 2016 | FRs | 6.89 | 51.3 | 95.0 | 8.42 | 24.0 | 3.34 | 1100 | -0.198 |
| | CRs | 7.12 (3.3%) | 64.3 (13%) | 94.6 (-0.4%) | 8.40 (-0.2%) | 20.1 (-3.9%) | 2.90 (-13.2%) | 1100 (0%) | -0.198 (0%) |
| | HRs | 7.38 (3.6%) | 70.1 (5.8%) | 93.4 (-1.2%) | 8.50 (1.2%) | 20.1 (0%) | 3.21 ^a (10.7%) | 1100 (0%) | -0.197 (-0.5%) |

^a Maximum storage during flood season of 2015 is lower than the upper bound of flood conservation ($1.68 \times 10^8 \text{ m}^3$). Maximum storage during flood season of 2016 is between the upper bound of flood water conservation ($1.68 \times 10^8 \text{ m}^3$) and upper bound of flood storage ($4.76 \times 10^8 \text{ m}^3$)

^{b, c} Percentages in parentheses indicate the indicator variation compared with results of FRs and CRs, respectively

6 Discussion

Parameters that reflect the forecast precision (σ_{ε_1} and σ_{ε_2}) could affect the HRs because of the influence on objectives and feasible ranges. The influence of each parameter is examined by comparing the results of experiments under three levels.

1. Standard deviation of the inflow forecast error during the refill phase (σ_{ε_1})

Different values of σ_{ε_1} were used to explore how the precision of the forecast changed. Three levels of σ_{ε_1} were selected and evaluated from the historical inflow forecast and observation samples according to best, medium, and worst forecast performance. The corresponding 3D-HR curves are shown in Fig. 6, with R_1 plotted as a function of A and \bar{T}_2 , and where the X-Y surface projection presents a traditional 2D depiction of HRs with scenarios of \bar{T}_2 .

The results verify the following.

1. The range of the flood water conservation zones decreased and narrowed as σ_{ε_1} increased for the HRs. The values of SWA and EWA reached $0.88 \times 10^8 \text{ m}^3$ and $1.07 \times 10^8 \text{ m}^3$, respectively, at the highest precision level ($\sigma_{\varepsilon_1} = 0.276 \times 10^8 \text{ m}^3$) (and they were attenuated to $0.51 \times 10^8 \text{ m}^3$ and $0.69 \times 10^8 \text{ m}^3$, respectively, at the lowest precision level ($\sigma_{\varepsilon_1} = 0.474 \times 10^8 \text{ m}^3$). This reflects the change in the HRs because of increases in the current-phase water release to mitigate any increase in the upstream flood risk caused by deterioration in the precision of the forecast.
2. HRs adjusted the current-phase release (R_1) at various levels of \bar{T}_2 and σ_{ε_1} with non-monotonic trends. In cases (a) and (b), for the HRs, R_1 increased with \bar{T}_2 and the flood water was maintained at a relatively low level because of the reduced water shortage risk during the pre-release phase. In case (c), the release was lower (higher conservation) on $\bar{T}_2 = 0.14 \times 10^8 \text{ m}^3$ than on $\bar{T}_2 = 0.34 \times 10^8 \text{ m}^3$. This is because the variation in σ_{ε_1} changed with the marginal upstream flood risk and altered the marginal water shortage risk. As σ_{ε_1} increased, the upstream flood risk distribution and the water shortage risk

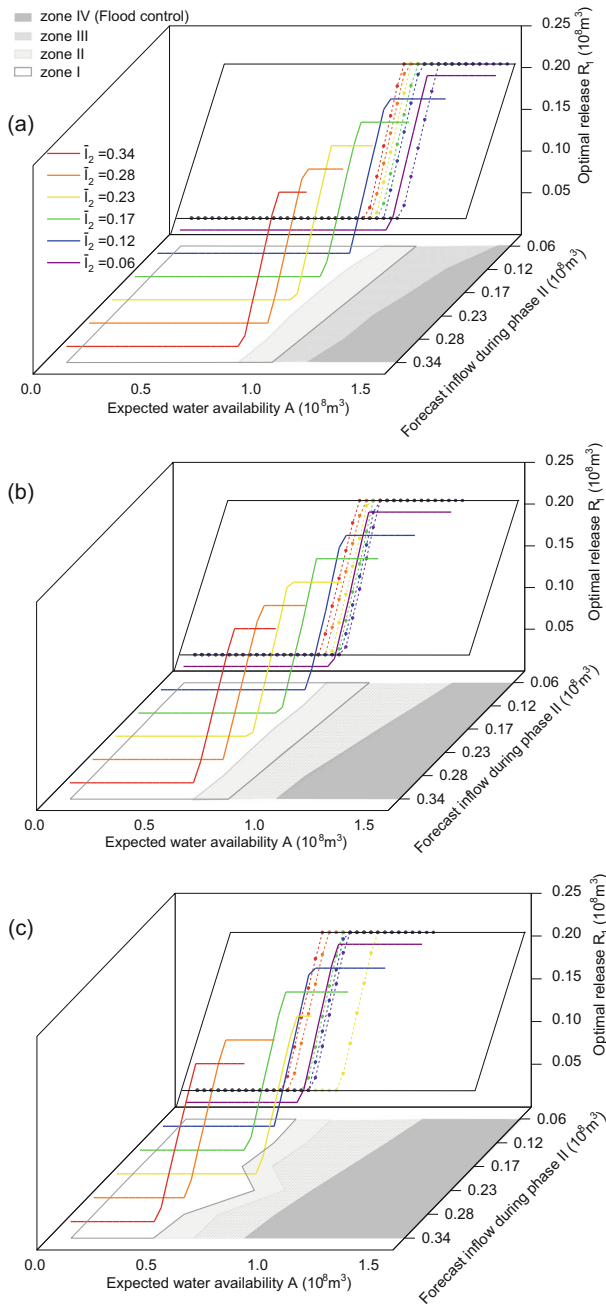


Fig. 6 HRs release (R_1) with expected water availability (A) and forecast inflows during the pre-release phase (\bar{I}_2) for σ_{ε_1} of (a) $0.276 \times 10^8 \text{ m}^3$, (b) $0.385 \times 10^8 \text{ m}^3$, and (c) $0.474 \times 10^8 \text{ m}^3$

distribution were flattened; the optimal release or conservation is therefore determined by the result of a non-monotonic balance influenced by the variation of the magnitude of the marginal risks.

3. The flood control zone enlarges as σ_{ε_1} increases. With the increase in σ_{ε_1} , both the EWA and the feasible range of flood water conservation shrink because the upstream and downstream flood risks are enhanced, indicating that the precision of the inflow forecast serves is important for conserving flood water.
4. Standard deviation of the inflow forecast error during the pre-release phase (σ_{ε_2}).

Under varied inflow forecast conditions during the pre-release phase, the value of σ_{ε_2} affects the HRs. Similarly, three levels of σ_{ε_2} were selected and evaluated from the historical samples, and the corresponding HRs graphs are plotted in Fig. 7.

The following can be concluded from the figures above.

1. For the HRs, the range of zones I and II were slightly enhanced and broadened as σ_{ε_2} increased. The values of SWA and EWA reached $0.66 \times 10^8 \text{ m}^3$ and $0.852 \times 10^8 \text{ m}^3$, respectively, at the highest precision level ($\sigma_{\varepsilon_2} = 0.45 \times 10^8 \text{ m}^3$) and increased to $0.68 \times 10^8 \text{ m}^3$ and $0.855 \times 10^8 \text{ m}^3$, respectively, at the lowest precision level. With the reduced precision of the inflow forecast within the pre-release phase, the reservoir potentially faces an intensified risk of water shortages, meaning that the increased chance of flood water conservation should be explored.
2. The current-phase release (R_1) determined by the HRs has an approximate monotonic variation with \bar{T}_2 and σ_{ε_2} . In each figure, it is clear that R_1 is increasingly enhanced as \bar{T}_2 increases, demonstrating a monotonic trend in the reduction of flood water conservation as \bar{T}_2 increases. Moreover, the HRs curves in Fig. 7a–c show that, as σ_{ε_2} increases, there was a monotonic reduction in R_1 . This was also attributed to the intensified influence of the reduced precision in the inflow forecast on the water shortage risk during the pre-release phase.

7 Conclusions

In this study, a two-phase optimal flood water conservation model for determining the HRs of reservoir operation during the pre-refill and pre-release phases was established. With the forecast error addressed as the major source of uncertainty within the model framework, optimal HRs for determining the best balance between upstream flood risk, downstream flood risk, and water shortage risk through flood water conservation were derived analytically, based on the first-order optimality condition. The Xianghongdian Reservoir was used as an example to explore the performance and sensitivity of the rules. The main findings from the study are as follows:

1. Optimal flood water conservation derived by the HRs determined the optimal balance between the upstream flood risk and water shortage risk to achieve the minimum total risk.
2. The HRs exhibit better flood water conservation performance in real-time operations for the HRs than the RFs and CRs without increasing the flood risk.
3. HRs for flood water conservation are strongly affected by the precision of forecasts. Generally, the conservation level increases when the precision of the forecast improves during the pre-refill phase, and decreases when the forecast precision improves during the pre-release phase.

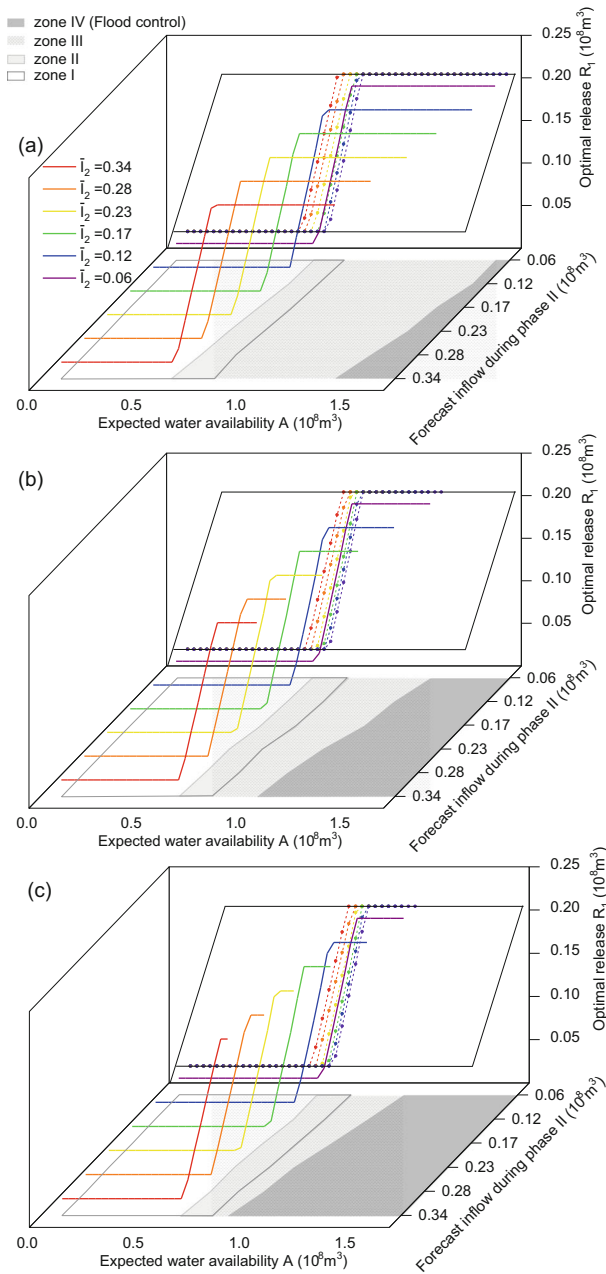


Fig. 7 HRs release (R_1) with expected water availability (A) and forecast inflows during the pre-release phase (\bar{I}_2) for σ_{ε_2} of (a) $0.45 \times 10^8 \text{ m}^3$, (b) $0.6 \times 10^8 \text{ m}^3$, and (c) $0.66 \times 10^8 \text{ m}^3$

Analytical two-phase HRs for flood water conservation through reservoir operation provide insights that allow the optimal conservation mechanism to be described through mathematical analysis. By satisfying the assumptions of two-phase model formulation, the proposed methodologies suit systems in which the flood risk is mainly determined by forecast errors in the

inflow quantity rather than in the inflow processes, particularly to regulate inflow variability in large reservoirs with high storage capacities. The study will be extended in the future to accommodate multi-phase feature analysis via stochastic optimization techniques, which will facilitate practical applications for a broad range of cases.

Acknowledgements We would like to thank three anonymous reviewers for their in-depth reviews and constructive suggestions. The remarks and summary of reviewer comments provided by the Editor and Associate Editor are also greatly appreciated, which have facilitated major improvements in this paper.

Funding Information This study is supported by National Key Technologies R&D Program of China (Grant No. 2017YFC0405604), the Fundamental Research Funds for the Central Universities (B200202028, B200202032), and the China Postdoctoral Science Foundation Funded Project (Grant No. 2018 T110525).

References

- Bayazit M, Unal NE (1990) Effects of hedging on reservoir performance. *Water Resour Res* 26(4):713–719
- Chou FNF, Wu C (2013) Expected shortage based pre-release strategy for reservoir flood control. *J Hydrol* 497: 1–14. <https://doi.org/10.1016/j.jhydrol.2013.05.039>
- Ding W, Zhang C, Peng Y, Zeng R, Zhou H, Cai X (2015) An analytical framework for flood water conservation considering forecast uncertainty and acceptable risk. *Water Resour Res* 51(6):4702–4726. <https://doi.org/10.1002/2015WR017127>
- Draper AJ, Lund JR (2004) Optimal hedging and carryover storage value. *J Water Res Plan Man* 130(1):83–87
- Hashimoto T, Stedinger JR, Loucks DP (1982) Reliability, resiliency, and vulnerability criteria for water resource system performance evaluation. *Water Resour Res* 18(1):14–20
- Hua L, Wan X, Wang X, Zhao F, Zhong PA, Liu M, Yang Q (2020) Floodwater utilization based on reservoir pre-release strategy considering the worst-case scenario. *Water-Sui* 12(3):892. <https://doi.org/10.3390/w12030892>
- Hui R, Lund J, Zhao J, Zhao T (2016) Optimal pre-storm flood hedging releases for a single reservoir. *Water Resour Manag* 30:5113–5129. <https://doi.org/10.1007/s11269-016-1472-x>
- Labadie JW (2004) Optimal operation of multireservoir systems: state-of-the-art review. *J Water Res Plan Man* 130(2):93–111
- Li X, Guo S, Liu P, Chen G (2010) Dynamic control of flood limited water level for reservoir operation by considering inflow uncertainty. *J Hydrol* 391(1–2):126–134. <https://doi.org/10.1016/j.jhydrol.2010.07.011>
- Liu S, Shi H (2019) A recursive approach to long-term prediction of monthly precipitation using genetic programming. *Water Resour Manag* 33(3):1103–1121. <https://doi.org/10.1007/s11269-018-2169-0>
- Lund JR, Guzman J (1999) Derived operating rules for reservoirs in series or in parallel. *J Water Res Plan Man* 125(3):143–153. [https://doi.org/10.1061/\(ASCE\)0733-9496\(1999\)125:3\(143\)](https://doi.org/10.1061/(ASCE)0733-9496(1999)125:3(143))
- Mao J, Tian M, Hu T, Ji K, Dai L, Dai H (2019) Shuffled complex evolution coupled with stochastic ranking for reservoir scheduling problems. *Wat Sci Eng* 12(4):307–318
- Moridi A, Yazdi J (2017) Optimal allocation of flood control capacity for multi-reservoir systems using multi-objective optimization approach. *Water Resour Manag* 31(14):4521–4538. <https://doi.org/10.1007/s11269-017-1763-x>
- Nayak MA, Herman JD, Steinschneider S (2018) Balancing flood risk and water supply in California: policy search integrating short-term forecast ensembles with conjunctive use. *Water Resour Res* 54(10):7557–7576. <https://doi.org/10.1029/2018WR023177>
- Shenava N, Shourian M (2018) Optimal reservoir operation with water supply enhancement and flood mitigation objectives using an optimization-simulation approach. *Water Resour Manag* 32(13):4393–4407. <https://doi.org/10.1007/s11269-018-2068-4>
- Shiau JT (2011) Analytical optimal hedging with explicit incorporation of reservoir release and carryover storage targets. *Water Resour Res* 47(1):W1515. <https://doi.org/10.1029/2010WR009166>
- Wan W, Zhao J, Lund JR, Zhao T, Lei X, Wang H (2016) Optimal hedging rule for reservoir refill. *J Water Res Plan Man* 142(11)
- Wen X, Liu Z, Lei X, Lin R, Fang G, Tan Q, Wang C, Tian Y, Quan J (2018) Future changes in Yuan River ecohydrology: individual and cumulative impacts of climates change and cascade hydropower development on runoff and aquatic habitat quality. *Sci Total Environ* 633:1403–1417. <https://doi.org/10.1016/j.scitotenv.2018.03.309>

- Xu B, Boyce SE, Zhang Y, Liu Q, Guo L, Zhong P (2017) Stochastic programming with a joint chance constraint model for reservoir refill operation considering flood risk. *J Water Res Plan Man* 143(1):4016067. [https://doi.org/10.1061/\(ASCE\)WR.1943-5452.0000715](https://doi.org/10.1061/(ASCE)WR.1943-5452.0000715)
- Xu B, Zhu F, Zhong P, Chen J, Liu W, Ma Y, Guo L, Deng X (2019) Identifying long-term effects of using hydropower to complement wind power uncertainty through stochastic programming. *Appl Energy* 253: 113535. <https://doi.org/10.1016/j.apenergy.2019.113535>
- Yang W, Norrlund P, Saarinen L, Witt A, Smith B, Yang J, Lundin U (2018) Burden on hydropower units for short-term balancing of renewable power systems. *Nat Commun* 9(1). <https://doi.org/10.1038/s41467-018-05060-4>
- Yeh WW (1985) Reservoir management and operations models: a state-of-the-art review. *Water Resour Res* 21(12):1797–1818. <https://doi.org/10.1029/WR021i012p01797>
- You J, Cai X (2008) Hedging rule for reservoir operations: I. A theoretical analysis. *Water Resour Res* 44(1):1–9. <https://doi.org/10.1029/2006WR005481>
- Zhang X, Liu P, Xu C, Gong Y, Cheng L, He S (2019) Real-time reservoir flood control operation for cascade reservoirs using a two-stage flood risk analysis method. *J Hydrol* 577:123954. <https://doi.org/10.1016/j.jhydrol.2019.123954>
- Zhao J, Cai X, Wang Z (2011) Optimality conditions for a two-stage reservoir operation problem. *Water Resour Res* 47(8):1–16. <https://doi.org/10.1029/2010WR009971>
- Zhao T, Zhao J, Lund JR, Yang D (2014) Optimal hedging rules for reservoir flood operation from forecast uncertainties. *J Water Res Plan Man* 140(12):4014041. [https://doi.org/10.1061/\(ASCE\)WR.1943-5452.0000432](https://doi.org/10.1061/(ASCE)WR.1943-5452.0000432)
- Zhou Y, Guo S, Liu P, Xu C (2014) Joint operation and dynamic control of flood limiting water levels for mixed cascade reservoir systems. *J Hydrol* 519:248–257. <https://doi.org/10.1016/j.jhydrol.2014.07.029>
- Zhu F, Zhong P, Xu B, Chen J, Sun Y, Liu W, Li T (2020) Stochastic multi-criteria decision making based on stepwise weight information for real-time reservoir operation. *J Clean Prod* 257:120554. <https://doi.org/10.1016/j.jclepro.2020.120554>

Publisher's Note Springer Nature remains neutral with regard to jurisdictional claims in published maps and institutional affiliations.

Affiliations

Bin Xu^{1,2} · Xin Huang¹ · Ping-an Zhong¹ · Yenan Wu³

Xin Huang
xinhuang@hhu.edu.cn

Yenan Wu
yenaw@ualberta.ca

¹ College of Hydrology and Water Resources, Hohai University, NO. 1, Xikang Road, Nanjing 210098, China

² Nanjing Hydraulic Research Institute, No. 223, Guangzhou Road, Nanjing 210029, China

³ Department of Civil and Environmental Engineering, University of Alberta, T6G2W2, Edmonton, Alberta, Canada